Applied Catalysis A: General 522 (2016) 80–89

Contents lists available at ScienceDirect

Applied Catalysis A: General

journal homepage: www.elsevier.com/locate/apcata

Coke promoters improve acrolein selectivity in the gas-phase dehydration of glycerol to acrolein

Marjan Dalil[a,*], Mahesh Edake[a], Camille Sudeau[a], Jean-Luc Dubois[b], Gregory S. Patience[a]

[a] Department of Chemical Engineering, Polytechnique Montréal, C.P. 6079, Succ. CV, Montréal, H3C 3A7 Québec, Canada
[b] ARKEMA, 420 Rue d'Estienne d'Orves, 92705 Colombes, France

ARTICLE INFO

Article history:
Received 15 February 2016
Received in revised form 20 April 2016
Accepted 21 April 2016
Available online 22 April 2016

Keywords:
Glycerol dehydration
Acrolein
Coke
HPW-TiO_2
Fluidized-bed
Coke-promoter

ABSTRACT

Commercial processes partially oxidize propylene to acrolein but glycerol can replace the petroleum derived feeds as a bio-feedstock for this large volume specialty chemical. Metal oxides, particularly acid catalysts, dehydrate glycerol at elevated temperature. Dehydration of glycerol to acrolein is usually performed in traditional fixed-bed reactors. We tested phosphotungstic acid (HPW) loaded on titania catalysts (a weight fraction of 10, 20 and 30%) at 280 °C in a fluidized-bed reactor. With time-on-stream, the acrolein selectivity increased and the coke selectivity decreased. As much as 85% of the glycerol formed coke in the first hour and less than 20% acrolein. We developed a new method to spray the liquid feed directly on the catalyst bed and the reaction occurred in the gas phase.

We also compared the performance of pure titania supports with respect to the acrolein selectivity. Acrolein selectivity was 13% higher on TiO_2 with an average pore diameter of 17.3 nm versus the TiO_2 support with a pore of 5.6 nm. Three times more coke formed on the small pore diameter TiO_2. We treated the catalyst with hydrogen rich coke promoters – tetralin and decalin – to passivate non-selective catalytic sites and to evidence hydrogen transfer reactions. This treatment increased acrolein selectivity from 10% to 30% in the first 30 min of reaction. As expected, they hydrogenated the intermediates to undesired compounds including acetone and propanaldehyde (propanal).

1. Introduction

Renewable feedstocks could replace petroleum to produce energy and chemicals. Researchers and industries endeavour to develop sustainable processes based on bio-resources. Adding biodiesel to petro-diesel is a first step to substitute petroleum fuel with bio-based fuels. Microalgae [1] and waste cooking oil [2] are possible large volume sources for biodiesel synthesis.

Glycerol is the main co-product of biodiesel synthesis (a mass fraction of 10%) and with the growing biodiesel industry the market has been overwhelmed resulting in low prices. Due to its multifunctional structure, glycerol is widely applied in various industries such as, food, cosmetics, pharmaceuticals and plastics. However, crude glycerol contains NGOM (non-glycerin organic matter), water, methanol and traces of fatty acids and must be purified. Distillation is an extra step in refining and thereby increases the cost of the process. Acrolein is versatile intermediate for the chemical industry and is a feedstock for acrylic acid and its esters, glutaraldehyde, methionine, polyurethanes and polyester resins [3–5]. The principal commercial process to synthesize acrolein relies on propylene as a feedstock and multi-tubular fixed bed reactors. Mixed-metal oxide containing Mo and Bi catalyses this reaction at 250–400 °C [6,7].

Due to the availability of glycerol from biodiesel synthesis, dehydration of glycerol to acrolein is a potential economic alternative to propylene oxidation. The early studies of glycerol dehydration were patented in 1930 by Kahlbum [8]. The yield of acrolein was 75% over lithium phosphate catalyst.

Synthesis of acrolein from glycerol has been studied in both gas and liquid phase reactions. Generally, gas-phase dehydration is preferred due to the environmental and operational issues of liquid-phase reactions.

Several classes of catalysts such as zeolites, mixed-metal oxides and heteropoly acids dehydrate glycerol to acrolein. Brønsted acids are active and selective in acrolein synthesis, but deactivation of the catalyst is the major drawback in this case. Dubois et al. [9] suggested in situ regeneration of the catalyst by co-feeding of molecular oxygen. They observed that molecular oxygen not

* Corresponding author.
E-mail address: marjan.dalil@polymtl.ca (M. Dalil).

http://dx.doi.org/10.1016/j.apcata.2016.04.022
0926-860X/

only decreased the coking rate, but also improved the acrolein selectivity. Additionally, the catalyst maintained its activity and reduced the by-products such as acetol and phenol. Few studies have focused on the effect of coke formation on catalyst performance. Erfle et al. [10] analysed used vanadium based catalysts by FTIR spectroscopy and concluded that coke forms on Brønsted sites. This conclusion was confirmed by Suprun et al. [11] who evaluated carbon deposits on phosphate catalysts. They also observed that higher reaction temperatures and small pore diameter of the catalyst lead to further carbon formation. Pethan Rajan et al. [12] characterized spent VPO by TPD-NH_3 and FTIR-pyridine. The results showed that the acidity and Brønsted acidic sites of the catalyst decreased after 40 h time-on-stream. Consequently, the conversion and selectivity of the catalyst decreased. The selectivity of acrolein over coked WO_3/TiO_2 catalysts is higher than on fresh catalyst and it remains active even after 6 h reaction time [13]. As a first step, we evaluated the performance of the coked catalyst and observed that partial regeneration of the catalyst improved the selectivity of acrolein and less coke formed in the early stages of reaction.

Although gas-phase dehydration of glycerol to acrolein has been studied since 1930 [8], most of the focus in this area is dedicated to fixed-bed reactors. Fixed-bed reactors are associated with some major drawbacks such as poor heat and mass transfer and hot spot formation in case of exothermic reactions. Considering the rapid deactivation of acid catalysts, catalyst regeneration is necessary in dehydration of glycerol. A fluidized bed reactor is the most suitable choice for this case as it provides a homogeneous heat and mass transfer and avoids local accumulation of the coke in catalytic bed.

Here, we tested three loadings of tungsten oxide over large pore and narrow pore titania supports. We focused on the effect of pore diameter on acrolein, by-products and coke selectivity. As preserving some coke on the surface of WO_3/TiO_2 improved acrolein selectivity in the first 15 min of reaction [13], we developed a novel method to treat our catalysts with hydrogen rich coke promoters such as tetralin and decalin to passivate non-selective sites of the catalyst and increase acrolein selectivity and to evidence the hydrogen transfer reactions taking place in the early phases of the reaction.

2. Methodology

2.1. Catalyst preparation

We prepared catalysts with a mass fraction of 10, 20 and 30% phosphotungstic acid ($H_3PW_{12}O_{40}$ or HPW) on large pore and narrow pore titania supports provided by ARKEMA (Hombikat 11010 – HKT-1 and Hombikat 11060 – HKT-2). A LA-950 (Horiba) laser diffractometer measured the particle size distribution (PSD) of the pure titania. The mean particle size of the supports was 95 μm and 106 μm for the HKT-1 and the HKT-2 samples, respectively. The HPW (Nippon Inorganic Color & Chemical Co., Ltd.) dissolved in 10 ml of distilled water in a rotavapor flask (BUCHI R-210). We subsequently loaded 10 g of titania to the flask. The rotavapor mixed the slurry for 2 h at room temperature. We applied a 60 mbar vacuum and heated the flask to 60 °C. The samples then dried for 10 h at 120 °C and calcined for 3 h at 500 °C [14].

2.2. Characterization techniques

An Autosorb-1 porosimeter (Quantachrome) measured the N_2 adsorption/desorption isotherms at −196 °C. We assigned the surface area based on the multi point BET (Brunauer, Emmett and Teller) equation and the pore size and pore volume of the samples on the BJH (Barrett–Joyner–Halenda) equation.

A TA-Q50 thermogravimetric analyzer measured the weight loss as a function of temperature. A Platinel II thermocouple placed 2 mm above the sample pan monitored the temperature. For each run, we loaded 20 mg of sample to a 10 μm aluminium crucible. The resolution and accuracy of the balance were 0.1 μg and >±0.1%.

A Philipps Xpert diffractometer scanned samples at room temperature (Cu anode, $K = 0.15406$ nm recorded the patterns at 50 kV voltage and 40 mA current) and produced the diffraction pattern (XRD) from which we deduced the HPW/TiO_2 crystal phases. The diffraction angle (2 theta range) varied between 20° and 90° at a 0.020° step size.

A JEOL JSM-7600TFE Field Emission Scanning Electron Microscopy recorded the microscopic images of the prepared catalysts. The samples were mounted on an aluminium sample holder containing a double graphite adhesive layer. We used both LEI (lower secondary electron image) and LABE (low-angle backscattered electron) detectors.

The samples prepared for FESEM analysis were also analysed at the same time for EDX imaging. An OXFORD (X-Max) instrument recorded the EDX images for elemental analysis of the samples.

For Fourier transform infrared spectroscopy (FTIR) a Spotlight 400 – PerkinElmer FTIR spectrometer was used. Prior to the analysis, the catalyst samples were treated with pyridine as the probe molecule. We recorded the background spectra of samples before analysing any samples. Then we treated the samples with pyridine at room temperature and desorbed the excess pyridine at 100 °C for 1 h. After cooling to room temperature, the instrument recorded the spectra. The IR range of the analysis was 600–4000 cm^{-1} with resolution of 16 cm^{-1}.

A heat flow calorimeter (Setaram C80) connected to a volumetric apparatus measured the acidity and basicity of the catalyst at 150 °C. The instrument was equipped with a Barocel capacitance manometer to monitor pressure. The probe molecules (ammonia for acidity and sulphur dioxide for basicity) were purified by successive freeze–pump–thaw cycles. First, 100 mg sample was pre-treated overnight at 250 °C under vacuum. To record the differential heats of adsorption, small doses of the adsorbate were introduced onto the catalyst and the pressure reached 66 Pa. The samples outgassed for 30 min at the same temperature, and the procedure was repeated at 150 °C and 27 Pa. The difference between the amounts adsorbed in the first and second steps represents the irreversibly adsorbed quantity (Virr) of a respective gas from which we estimate the number of acidic/basic sites.

2.3. Experimental

2.3.1. Catalytic reaction set-up

HPW/TiO_2 catalysts dehydrated glycerol in a quartz fluidized-bed reactor. The reactor height was 52 mm and its inner diameter was 8 mm. A 20 μm ceramic frit distributed the gas uniformly across the reactor. Fluidized-beds are ideal reactors to regenerate catalysts: the high solids mixing rate minimizes thermal and concentration gradients. In fixed bed reactors, coke may build up on catalysts preferentially at the entrance of the reactor and in the central region, which complicates interpreting reaction kinetics [15]. A three-zone furnace heated the reactor and a thermocouple 100 mm above the distributor monitored the bed temperature (Fig. 1).

A mixture of argon and oxygen fluidized the catalyst. To determine the minimum fluidization velocity (U_{mf}), we recorded the pressure drop at ascending and descending gas flow rates (Fig. 2a). The U_{mf} of all samples was 1.4 cm s^{-1}. The total gas velocity was held three times higher than this value for all the experiments.

The molecular oxygen (a mixture of 21 mol% O_2/Ar) co-fed with glycerol to maintain the catalyst life time and increase acrolein selectivity while decreasing aromatic and hydrogenated by-products [9,13].

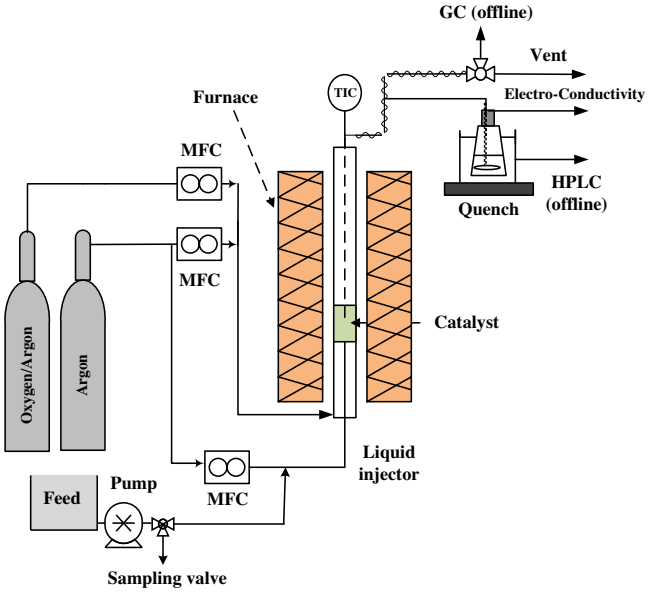

Fig. 1. Diagram of experimental set-up for dehydration of glycerol. Glycerol was injected above the grid as shown in our previous publication [13].

An HPLC pump injected the glycerol aqueous solution (28 wt% glycerol in water, flow rate: 0.5 ml min^{-1}) directly into the fluidized-bed of catalyst. It should be noted that the reaction conditions were selected to evidence the transient phenomena during the initial phase of catalytic reaction. The liquid feed entered the reactor through a 1.6 mm nozzle without preheating. A flow of argon assisted the liquid feed to enhance the quality of liquid spray. The volumetric ratio of argon/glycerol solution was constant (200) for all the experiments. To ensure that the droplets were uniform, we tested the injector with a series of gas/liquid ratios. Large droplets agglomerate the catalyst and block the injector. The flow of Ar in the injector should be high enough to spray the liquid feed into the catalyst bed but too high flow rate attrits the catalyst.

The effluent gases from the reactor passed through two quenches to trap all the condensable compounds. A Hanna electrical conductivity meter monitored the product quench (first quench); the conductivity is correlated to the concentration of ionizable solutes. The concentration of the liquid products trapped in the quench increased with reaction time. Using the conductivity meter we were able to monitor and follow the production rate by reaction time (Fig. 2b).

A Bruker GC (equipped with Hyesep Q, Molsieve 5A and FFAP columns) analysed the gas and liquid products (Fig. 1).

The conversion of glycerol ($X_{gly.}$) as well as products selectivities (S_p) were calculated as follows;

$$X_{gly.}\,(\text{mol\%}) = \frac{n^{in}_{gly.} - n^{out}_{gly.}}{n^{in}_{gly.}} \times 100 \quad (1)$$

$$S_p\,(\text{mol\%}) = \frac{n_p}{n^{in}_{gly.} - n^{out}_{gly.}} \times \frac{z_p}{z_{gly.}} \times 100 \quad (2)$$

where $n^{in}_{gly.}$ and $n^{out}_{gly.}$ are the molar flow rates of glycerol at reactor entrance and exit. In Eq. (2), n_p is the molar stream of each product. z_p and $z_{gly.}$ represent the number of carbon atoms of the products and glycerol.

3. Results and discussion

3.1. Catalyst characterization

3.1.1. N_2 adsorption/desorption

The surface area of pure HKT-1 TiO_2 was 71 $m^2\,g^{-1}$, whereas the average pore diameter and total pore volume were 17 nm and 0.22 $cm^3\,g^{-1}$. The HKT-2 TiO_2 surface area was 148 $m^2\,g^{-1}$ with the same pore volume. The average pore diameter, however, was three times smaller than HKT-1 titania (5.6 nm). The tungsten loading and calcination affected the physiochemical properties of TiO_2: both surface area and pore volume dropped as the tungsten loading increased: tungsten covers the surface and partially fills the pores. These properties for calcined samples were lower still. The surface area of TiO_2 dropped by 70% for HKT-1 and by 40% for HKT-2, when loaded with 30% HPW and calcined (Table 1).

Knowing that Keggin unit covers 1.2 nm^2, we calculated the theoretical coverage of the pure TiO_2 by HPW. On HKT-1 titania with a surface area of 71 $m^2\,g^{-1}$, for a monolayer coverage, 22 wt% loading is needed. On the other hand, for HKT-2 titania with a surface area of 148 $m^2\,g^{-1}$, the loading of 37 wt% is required to create a monolayer. This explains the higher drop in the surface area of HKT-1 rather than HKT-2. We can also conclude that with HKT-2 one can have a higher tungsten loading before a drop in surface area rather with HKT-1; because HPW adsorbs on the surface until a monolayer coverage is reached.

Pore volume also decreased by 80% and 40% for HKT-1 and HKT-2, respectively but the pore diameter remained constant. Calcination impacts pore volume of the catalysts which can be correlated to the changes in phases.

3.1.2. X-ray diffraction

The X-ray diffraction patterns of fresh TiO_2 (HKT-1, HKT-2) and 30% HPW/TiO_2 suggested that the synthesized catalysts are crystalline (Fig. 3). All samples exhibited main relative peaks (101, 004,

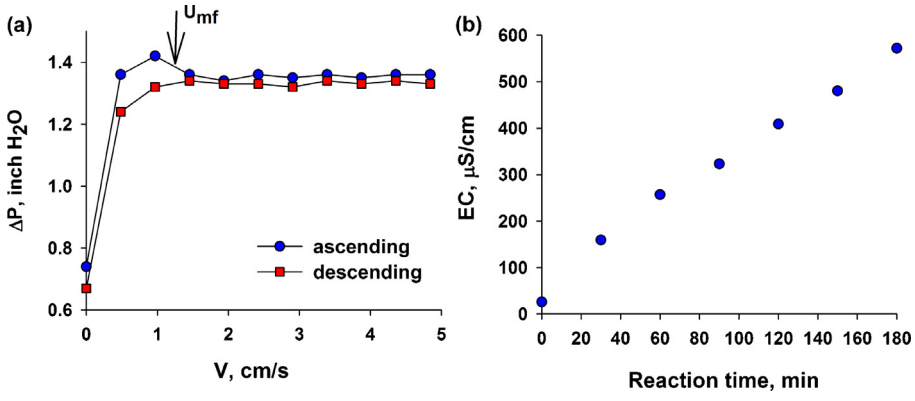

Fig. 2. (a) Minimum fluidization graph, (b) concentration of product mixture increased as reaction continued.

Table 1
Textural properties of various HPW/TiO_2 catalysts.

Sample	SA ($m^2\ g^{-1}$)		υ_p ($cm^3\ g^{-1}$)		d_p (nm)	
	Not-calcined	Calcined	Not-calcined	Calcined	Not-calcined	Calcined
Pure TiO_2 (HKT-1)	71	–	0.22	–	17	–
10% HPW/HKT-1	68	64	0.19	0.17	17	17
20% HPW/HKT-1	38	33	0.12	0.10	17	17
30% HPW/HKT-1	25	22	0.08	0.05	17	17
Pure TiO_2 (HKT-2)	148	–	0.20	–	6	–
10% HPW/HKT-2	144	137	0.20	0.18	5	5
20% HPW/HKT-2	121	119	0.18	0.15	5	5
30% HPW/HKT-2	92	88	0.14	0.12	5	5

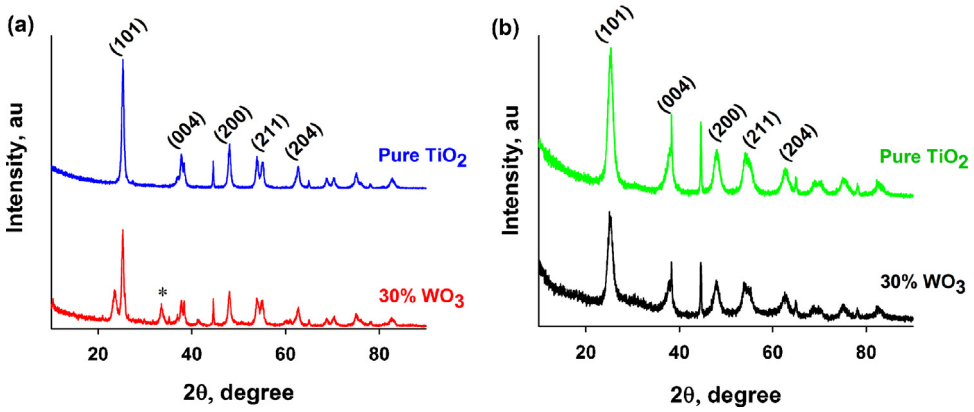

Fig. 3. XRD patterns for pure titania and 30% loading of HPW on (a) HKT-1 and (b) HKT-2 supports. *Crystalline phase of WO_3.

200, 211, 204) of the anatase form of TiO_2. We attributed the peaks at 23.4°, 37.6°, 54.5° and 67.2° to crystalline tungsten oxide peaks.

Although calcination could decompose the heteropoly acid (HPW), in the presence of water vapor HPW could be reconstructed from dispersed metal oxides. However, the characteristic peak of Keggin type phosphotungstic acid was not observed in the XRD pattern of calcined catalysts.

In Fig. 3a, the peak at 33.7° represents the crystalline phase of WO_3. On the other hand, 30%HPW/ HKT-2 catalyst did not show characteristic peaks of W oxide (Fig. 3b), which indicates that HPW clusters were well dispersed on the support with higher surface area (Table 1) and a monolayer coverage would be reached at higher tungsten loading. As mentioned before, for a monolayer coverage over HKT-1 titania, 22 wt% loading of HPW is required. For HKT-2 titania, on the other hand, a loading of 37 wt% is needed to create a monolayer. This explains the appearance of WO_3 peaks for HKT-1 in the XRD pattern. However, the peak intensities of both supports decreased when tungsten was loaded on titania [16,17].

3.1.3. Morphology-FESEM

The high magnification images of the uncalcined and calcined HPW/TiO_2 (FE-SEM) show that they are spheroidal (Fig. 4) and their diameter varied between 80 μm and 120 μm. The surface was rough. Calcining the catalyst improves the catalytic activity and may distribute the HPW over the TiO_2 since fewer micro-domains of HPW are present on calcined samples (white dots on spheres in Fig. 4). Catalyst assemblies were closely packed and marginal cracks appeared on the grain surfaces of the calcined samples. The cracks might be formed due to the high capillary pressure generated during the impregnation process that manifest themselves when the

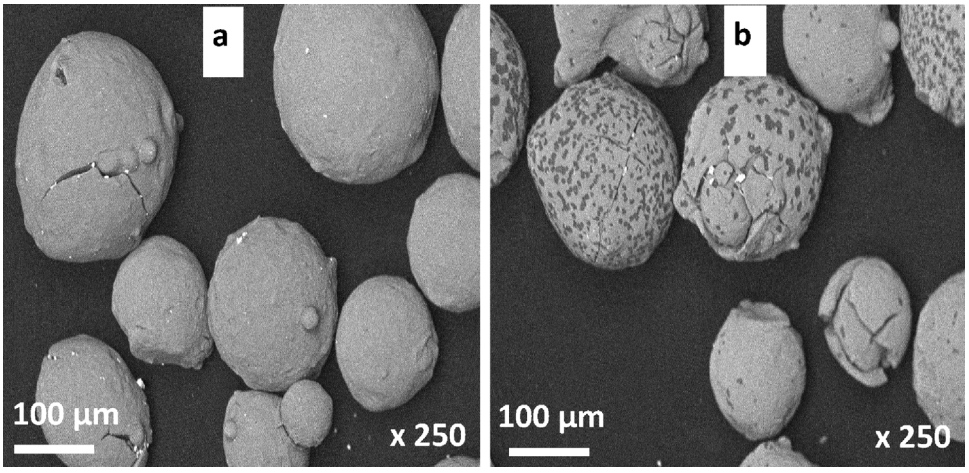

Fig. 4. FE-SEM images of (a) uncalcined and (b) calcined 30% HPW on HKT-1 supports.

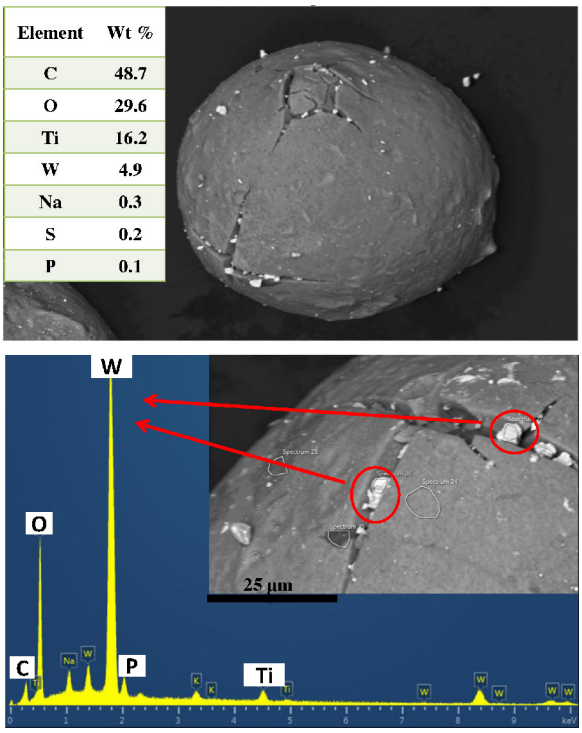

Fig. 5. Elemental composition of 30% HPW/TiO_2 catalyst.

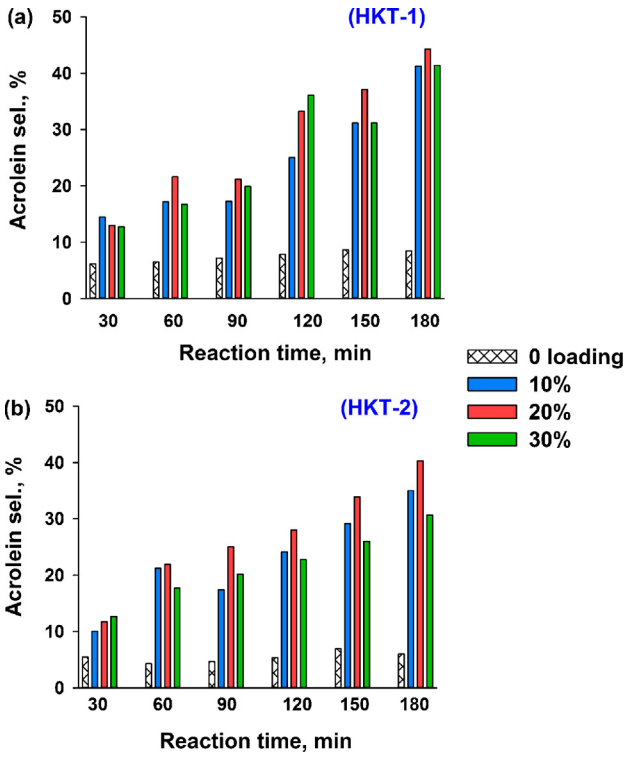

Fig. 6. Selectivity of acrolein over 10%, 20% and 30% of HPW on (a) HKT-1 and (b) HKT-2 titania supports.

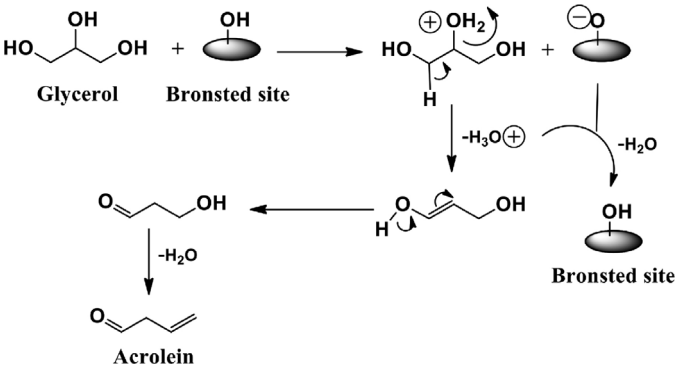

Fig. 7. Mechanism of glycerol dehydration over Brønsted sites proposed by Kinage et al. [23].

catalyst is heated. The cracks were less visible on fresh catalyst which may have formed during spray drying.

Energy dispersive X-ray spectroscopy (EDX) confirmed the presence of W and Ti elements in the calcined catalysts (Fig. 5). The dispersion of tungsten on titania is also shown in Fig. 5. According to the EDX results for 30 wt% HPW/TiO_2, the weight ratio of W:Ti is 0.3, which is consistent with our calculations for the preparation procedure.

3.2. Catalytic reaction over HPW/TiO_2 samples

We tested the performance of all the catalysts to determine the effect of tungsten loading on product selectivity. We loaded the reactor with 1.5 g of catalyst and heated the catalyst bed to 280 °C. The molar ratio of the gas feed was: glycerol/O_2/H_2O/Ar: 0.1/0.01/0.25/0.33. The GC analysed both liquid and gas samples that we collected every 30 min.

3.2.1. Effect of HPW loading on acrolein selectivity

Every catalyst containing tungsten converted all the glycerol, even in the first 30 min. However, the conversion of glycerol over pure HKT-1 and HKT-2 was only 65% and 54%, respectively. Both titania supports, containing 20% HPW, produced more acrolein than 10% and 30% catalysts and the maximum acrolein selectivity was 48%, (20% HPW on HKT-1 titania). Regardless of the reaction time, the lowest acrolein yield, on the other hand, was over pure titania samples (Fig. 6). Pure HKT-1 and HKT-2 titania produced only 8% and 6% acrolein.

Low glycerol conversion and acrolein selectivity over pure titania catalysts are attributed to the presence of basic (medium and weak [18]) and Lewis acid sites in TiO_2 [18]. Lewis sites on the surface of pure TiO_2 may react with steam and generate Brønsted sites [19]. Foo et al. [20] proved that Brønsted acid sites can be formed from Lewis sites in the presence of water vapor. According to their FTIR-pyridine results, the concentration of Lewis acid sites on Nb catalyst decreased when the catalyst was exposed to water vapor at 350 °C. The number of Brønsted sites, on the other hand increased.

Acrolein is formed over strong Brønsted sites [9,18,19,21,22]. Impregnating HPW over pure titania increased catalysts acidity and produced Brønsted sites [18] which favour acrolein selectivity. Brønsted acid protonates the central hydroxyl group of glycerol to release a water molecule and a proton from glycerol. The resulting intermediate, 3-hydroxypropanal, further dehydrates to acrolein (Fig. 7).

On pure titania surface, basic sites control the non-selective reaction pathway. To improve the catalyst, not only Brønsted sites should be available on the surface, but also the concentration of HPW species should be high enough to cover the non-selective sites of the support. Stosic et al. [18] established a correlation between the number of acid/base sites of the catalyst and acrolein selectivity. According to SO_2 adsorption results, pure titania showed basic characteristics and as the loading of HPW increased, basicity of titania decreased as well. Furthermore, as the number of basic sites increased, the selectivity of acrolein decreased. 10 wt% tungsten was insufficient to create a monolayer coverage and passivate the

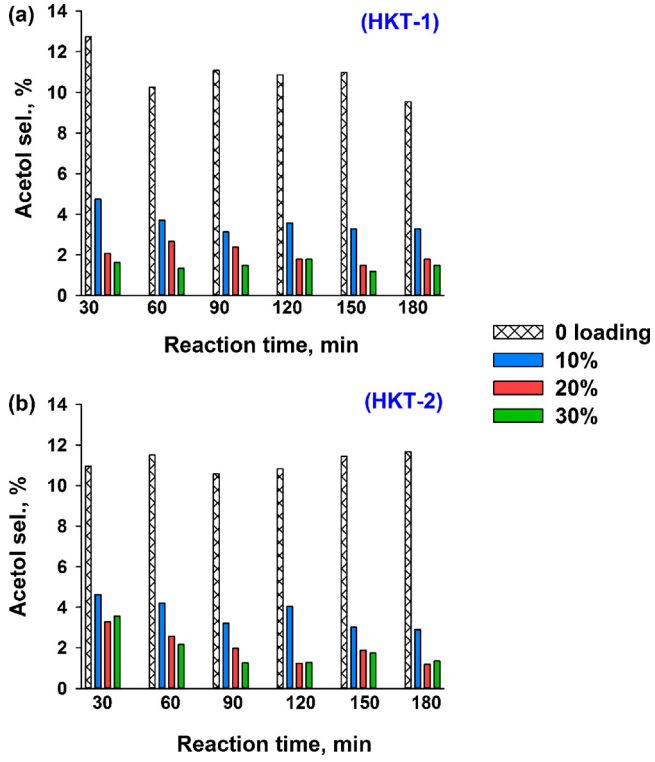

Fig. 8. Selectivity of acetol over 10%, 20% and 30% of HPW on (a) HKT-1 and (b) HKT-2 titania supports.

non-selective sites so more tungsten was required (for a monolayer coverage on HKT-1, 22 wt% of HPW and on HKT-2, 37% HPW is required). On the other hand, adding too much tungsten will form HPW crystals and thereby reduce acrolein selectivity.

3.2.2. *Effect of tungsten loading on by-products*

The major by-products were acetol, acetaldehyde, formic acid, propanal and acetone. The selectivity of acetol decreased in the order of: pure TiO_2 > 10% > 20% > 30% (Fig. 8). Selectivity towards acetol was higher when pure titania catalysed the reaction. It was 9% for HKT-1 and 11% for HKT-2 titania. Adding 10% HPW to titania, dropped the selectivity to 3% (Table 2). The acid/base properties of titania account for the differences in glycerol conversion and product distribution.

Acetol could be formed over basic sites of titania [18]. A possible route for the reaction over basic sites starts with the dehydration of terminal hydroxyl groups resulting in the formation of enol intermediate, which can further undergo rapid rearrangement to acetol [18].

3.2.3. *Effect of TiO_2 support on product distribution*

The activity of the HKT-1 titania sample (large pore) was higher than that of HKT-2 (smaller pore) (Table 2). The performance of 20 wt% samples was compared in order to study the effect of titania support in acrolein production. Catalysts prepared with HKT-1 were more selective towards acrolein compared to those based on HKT-2 and after 3 h, they produced 10% more acrolein (44% for HKT-1 vs. 34% HKT-2). The formation of by-products did not vary significantly as we changed the TiO_2 support. Higher acrolein selectivity could be attributed to the difference of the average pore diameter of the two titania supports (Table 1) and confirms the results of the previous works [14,24].

The pore diameter of HKT-1 is three times larger than that of HKT-2. Therefore, HKT-1 provides more space within its pores for the reactants and the active phase metal to react. Tsukuda et al. [25] and Atia et al. [26] reported the same effect of pore size distribution on acrolein yield for silica heteropoly acids.

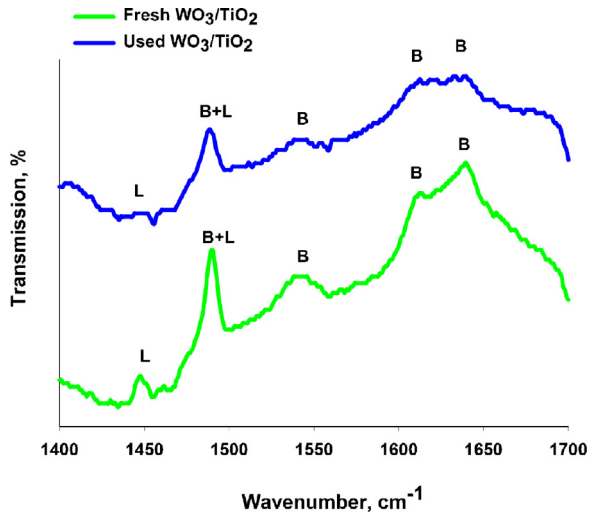

Fig. 9. FTIR spectra recorded after pyridine adsorption at room temperature and desorption at 100 °C for fresh and used catalysts.

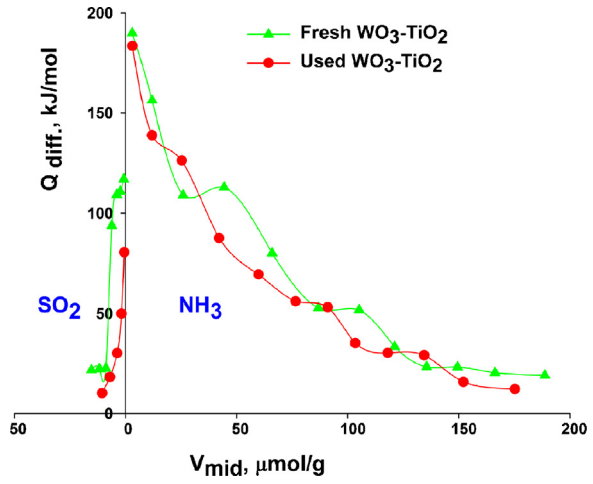

Fig. 10. Differential heats of NH_3 and SO_2 adsorption as a function of surface coverage for fresh and used WO_3/TiO_2 catalyst after 2 h.

The acrolein selectivity increased with time-on-stream [13]. Increasing trend for acrolein selectivity with reaction time is related to the formation of coke on non-selective sites of WO_3/TiO_2.

We performed FTIR pyridine analysis for fresh and used catalysts collected during an extended experiment (6 h). We observed that by reaction time, the band at 1450 cm^{-1} corresponding to the Lewis sites of the fresh catalyst disappeared while the peaks related to Brønsted acid sites were only reduced. However, for the used catalyst, Brønsted acidity was still dominant even after 6 h indicating that the catalyst was still selective towards acrolein. This also proves that Lewis acid sites did not contribute to acrolein selectivity (Fig. 9).

Microcalorimetric results showed that fresh catalyst adsorbed the most ammonia (86.5 $\mu mol\,g^{-1}$) because it has most acid sites and the highest strength (high heats of adsorption). As coke forms, the catalyst adsorbs fewer probe molecules and after 2 h of reaction, the adsorbed ammonia (acidity) was reduced to 64.3 $\mu mol\,g^{-1}$. We also observed that coke formation reduces the number of medium and weak acid sites while the number of strong acid sites did not vary by coke formation (Fig. 10). This explains why with reaction time the catalyst remained fully active and produced acrolein.

Table 2
Selectivity of the products in dehydration of glycerol at 280 °C after 3 h time-on-stream.

Sample	Conversion	$S_{acrolein}$	$S_{propanal}$	$S_{acetone}$	$S_{acetaldehyde}$	$S_{formic\ acid}$	S_{acetol}
Pure TiO_2 (HKT-1)	65.0	8.5	1.5	3.3	3.7	3.2	9.5
10 wt% HPW/HKT-1	96.0	41.3	1.0	2.3	1.6	2.2	3.3
20 wt% HPW/HKT-1	100	48.3	2.0	2.0	2.0	1.4	1.8
30 wt% HPW/HKT-1	100	41.4	1.5	2.0	2.4	1.6	1.5
Pure TiO_2 (HKT-2)	54.2	6.0	2.6	3.7	3.0	3.2	11.7
10 wt% HPW/HKT-2	100	33.0	1.7	1.7	2.2	2	2.9
20 wt% HPW/HKT-2	100	35.3	2.5	1.0	2.6	1.8	1.2
30 wt% HPW/HKT-2	100	31.6	2.5	1.0	2.1	2	1.3

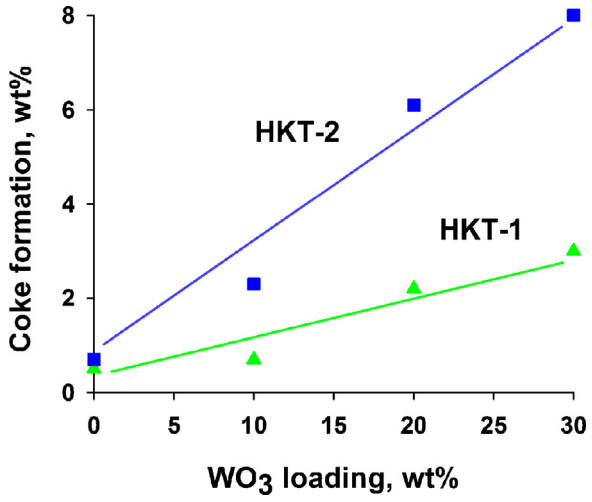

Fig. 11. Coke deposition over different HPW/TiO_2 catalysts after 3 h. Smaller pore diameter and high loading of HPW increased the coke formation.

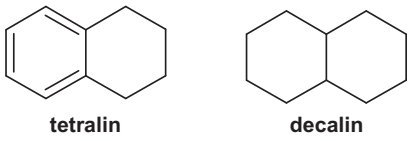

Fig. 12. Tetralin: $C_{10}H_12$ and decalin: C_10H_18 used as coke promoters to coat HPW/TiO_2 catalysts.

Table 3
TGA results measured the weight loss of the treated catalysts caused by the addition of tetralin and decalin.

Sample	Hydrocarbon	Weight gain (wt%)
20 wt% HPW/HKT-1	Tetralin	3.5
20 wt% HPW/HKT-1	Decalin	3.5
20 wt% HPW/HKT-2	Tetralin	3.9
20 wt% HPW/HKT-2	Decalin	3.7
WO_3/TiO_2 (ARKEMA)	Tetralin	3.6
WO_3/TiO_2 (ARKEMA)	Decalin	3.5

According to the SO_2 adsorption measurements for basicity evaluations, fresh catalyst has also basic characteristic of medium to weak strength (SO_2 adsorption of 3.8 μmol g^{-1}). The basicity decreased to 2.2 μmol g^{-1} after 2 h, as coke accumulates on the surface. Thus the changes in acidity and basicity of the catalyst caused by coke formation relate to the acrolein selectivity.

3.2.4. Coke

To quantify the mass of coke on the catalyst surface, we heated the sample in a TGA and measured the weight loss [13]. Coke deposition after 3 h was 0.5 wt% for pure HKT-1 and 0.7 wt% for HKT-2; it reached to 3 wt% and 8 wt%, respectively with 30 wt% tungsten. For both supports, as we increased the loading of HPW, more coke formed (Fig. 11). According to Yang et al. [16] and Chai et al. [27], HPW on pure titania increases the acidity and as a result more coke accumulates.

Coking was higher on the HKT-2 compared to HKT-1 (Fig. 11). Smaller pores (Table 1) are responsible for the higher coke levels. This observation confirms the results reported by Possato et al. [28] about the effect of pore diameter of MFI zeolite on coke formation.

Glycerol can condense in the pores (capillary condensation). This is favoured when the temperature is low, pores are too narrow and glycerol concentration is rather high (28 wt% in water) [29]. The diffusion limitations (steric limitations) could inhibit the effective desorption of the reactants and the products in catalyst framework.

3.2.5. Catalyst treatment with coke promoters

During the first hour of glycerol dehydration, coke selectivity was highest and the acrolein selectivity was lowest. With time-on-stream less coke formed as well as the hydrogenated by-products such as acetone, but the acrolein selectivity increased. Partially regenerated catalyst increased the acrolein selectivity from 10% to 25% in the first 15 min due to the coverage of the non-selective sites by coke [13]. We chose tetralin and decalin as "coke promoters" because these compounds are rich in hydrogen and carbon (Fig. 12). We were following two objectives by coating the catalysts with decalin and tetralin; first, to reach higher selectivity of acrolein in the initial phase of reaction and second, to see the effect of various coke promoters on products formed through the hydrogen transfer reactions.

Tetralin and decalin have similar boiling points but very different melting points. We spread 10 g of catalyst in a porcelain dish and placed it inside a desiccator. In a separate plate, inside the desiccator, we placed 10 g of hydrocarbon and heated the system to 120 °C in an oven. After 1 h, the colour of the catalyst turned to dark grey indicating that the product evaporated and adsorbed on the catalyst surface. We used three different catalysts: 20 wt% phosphotungstic acid on HKT-1 and HKT-2 titania as well as WO_3/TiO_2 catalyst (ARKEMA, as prepared in Ref. [14]).

To assure that the catalyst contained tetralin and decalin under the reaction condition, the TGA measured the quantity of the hydrocarbon deposited on catalyst. First, we heated the samples to 270 °C (ramp: 10 °C min^{-1}) with 40 ml min^{-1} nitrogen. After a 15 min isothermal hold, oxygen substituted the nitrogen and we ramped the temperature to 450 °C and measured the weight loss of the samples in TGA. At this point there was 3.5–3.9% hydrocarbon on the catalyst (Table 3) – each catalyst adsorbed about the same mass of hydrocarbon.

The performance of coated samples was compared to the original catalysts under the same reaction conditions. We loaded the reactor with 1 g of catalyst and operated at 270 °C. The temperature was purposely held rather low to avoid the decomposition of tetralin and decalin. Each reaction continued for 2 h. Meanwhile, we collected gas and liquid samples every 30 min and measured their concentration by GC.

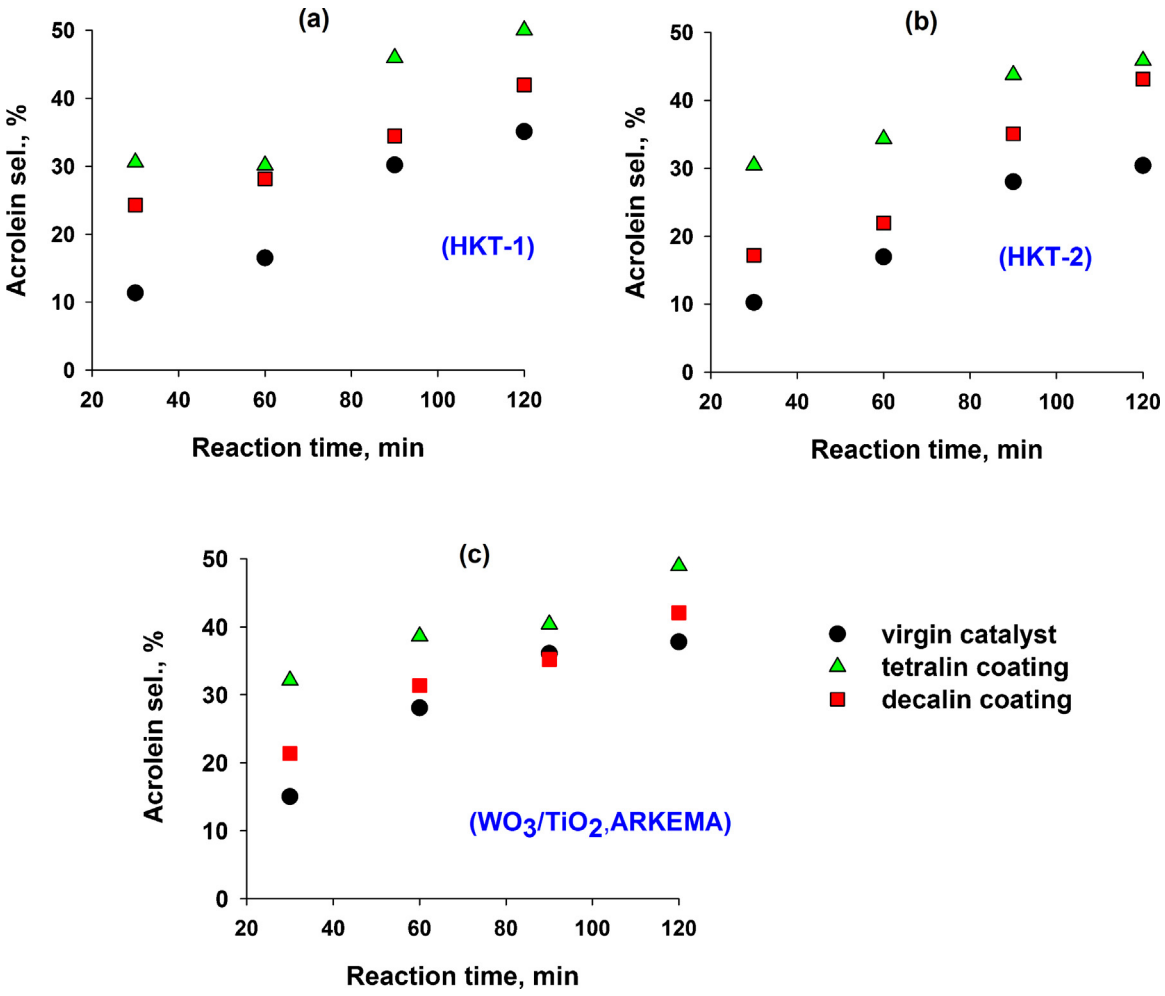

Fig. 13. Adding tetralin and decalin to HPW/TiO_2 catalysts increased the selectivity of acrolein at 270 °C. (a) and (b) correspond to the catalysts supported on HKT-1 and HKT-2 titanias, respectively. (●) 20 wt% HPW/TiO_2, (▲) decalin and (■) tetralin treated samples.

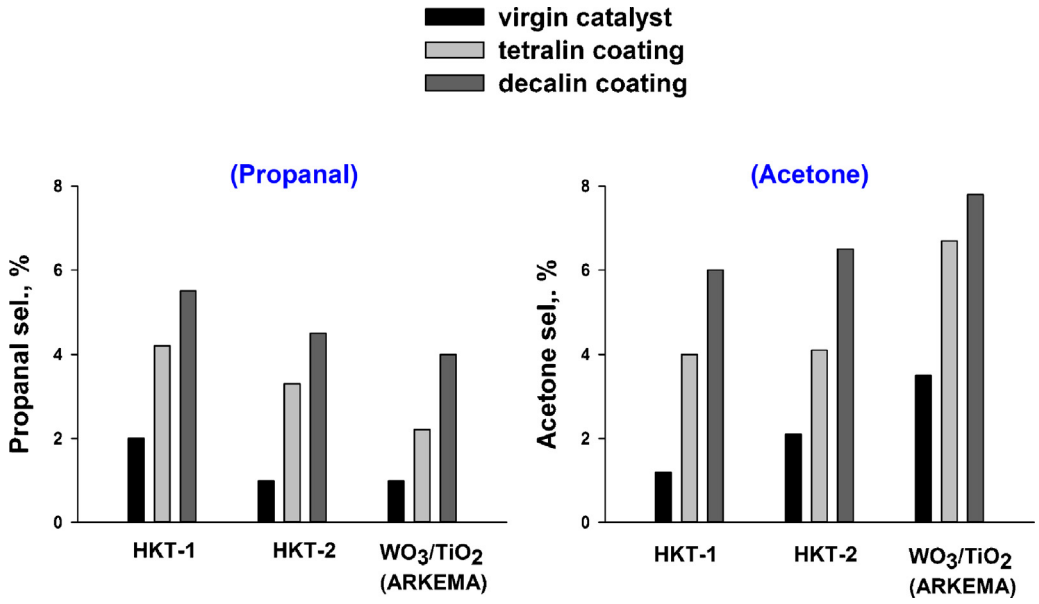

Fig. 14. Selectivity of propanal and acetone at 2 h for virgin and coated catalysts; addition of tetralin and decalin to HPW/TiO_2 catalysts, increased the selectivity of hydrogenated by-products at 270 °C.

Table 4
Product distribution of glycerol dehydration at 2 h over coated HPW/TiO_2 catalysts.

Sample	Treatment	Conversion	$S_{acrolein}$	$S_{propanal}$	$S_{acetone}$	$S_{acetaldehyde}$	$S_{formic\ acid}$	S_{acetol}
HPW/HKT-1	–	92.5	35.2	2.0	1.2	1.5	1.4	2.6
HPW/HKT-1	Tetralin	90.3	50.1	4.2	4.0	2.0	0.6	3.5
HPW/HKT-1	Decalin	90.0	42.0	5.5	6.0	1.0	1.5	3.0
HPW/HKT-2	–	88.6	30.4	1.0	2.1	1.0	1.8	2.5
HPW/HKT-2	Tetralin	87.8	45.8	3.3	4.1	1.2	2.1	3.0
HPW/HKT-2	Decalin	88.5	43.2	4.5	6.5	2.3	1.4	3.2
WO_3/TiO_2 (ARKEMA)	–	92.0	37.8	1	3.5	2.0	0.9	3.6
WO_3/TiO_2 (ARKEMA)	Tetralin	92.0	49.0	2.2	6.7	2.5	1.3	3.0
WO_3/TiO_2 (ARKEMA)	Decalin	89.7	42.1	4.0	7.8	2.3	1.3	2.0

3.2.6. *Effect of coke promoters on acrolein selectivity*

Adding coke promoters to HPW/TiO_2 catalysts increased acrolein selectivity. After 30 min, over 20 wt% HPW/HKT-1 catalyst, acrolein selectivity increased from 10% to 24% for decalin and to 30% for tetralin treated samples. Acrolein selectivity was 10% for untreated 20 wt% HPW/HKT-2 and reached to 30% and to 17% when tetralin and decalin were added, respectively. Acrolein selectivity doubled for tetralin treated WO_3/TiO_2 (ARKEMA) samples and it increased from 15% to 21% when decalin was used as coke promoter.

For virgin catalysts, more coke formed than acrolein and by-products at the beginning of reaction. With time, the selectivity of acrolein increased and the coke selectivity decreased considerably [13]. Coke built-up on the catalyst and passivated non-selective sites. Coke promoters substituted severe coke formation in the first 30 min and the active sites of the catalyst which were selectively producing coke or by-products, were covered by large molecules of tetralin and decalin (Fig. 13).

3.2.7. *Effect of coke promoters on by-products formation*

The selectivity of propanal and acetone increased over the catalysts treated with tetralin and decalin. This could be related to the high quantity of hydrogen in these compounds that become hydrogen donors. Propanal and acetone are both hydrogenated products and formed through hydrogen transfer. Acrolein hydrogenates to propanal and glycerol dehydrates to acetol. Acetol hydrogenates to 1,2-propanediol, which can further dehydrate to acetone (Fig. 14). The selectivity of both propanal and acetone dropped with time (as the hydrogen donor capacity of the tetralin and decalin dropped) but the selectivity of acetaldehyde, formic acid and acetol was constant (Table 4).

These results confirm that it is important to keep some coke on the catalyst surface, and that a dehydrogenated coke is better for acrolein selectivity. Note that hydrogenated side products are more important when decalin is used instead of tetralin, since it has more hydrogen available.

4. Conclusions

The price of glycerol has dropped due to its overproduction from biodiesel synthesis. Commercial dehydration of glycerol to acrolein is an economic alternative to propylene oxidation if catalysts can achieve high acrolein selectivity and resist rapid deactivation. The titania support pore size affects the acrolein selectivity and coke: three times more coke formed in the small pore diameter titania due to glycerol capillary condensation. Acrolein selectivity reached 48% with 20 wt% HPW at 280 °C. Coke passivates some non-selective sites, which we demonstrated with tetralin and decalin as coke promoters. Furthermore, acrolein selectivity increases with time-on-stream as the coke accumulates on the catalyst. In a continuous process, it is then important to keep a constant level of coke for which the fluidized-bed reactors are most suitable as they provide a homogeneous mass and heat distribution and avoid the formation of hot spots and local accumulation of coke. In conventional multi-tubular reactors, oxygen (in a regeneration step) will combust all the coke progressively from the entrance to the exit of the bed. If all of the coke combusts, the acrolein selectivity will be low when the reactor switches from regeneration to glycerol dehydration. Partially regenerating [13], distributing the O_2 supply [30] and reverse flow regeneration [31] may mitigate the non-selective reactions.

Acknowledgements

The authors would like to thank Natural Sciences and Engineering Research Council of Canada (NSERC), Canadian Foundation for Innovation (CFI), CRIBIQ and Mitacs for their financial support of this study.

References

[1] M.Y. Menetrez, Environ. Sci. Technol. 46 (13) (2012) 7073–7085.
[2] G.L. Maddikeri, A.B. Pandit, P.R. Gogate, Ind. Eng. Chem. Res. 51 (45) (2012) 14610–14628.
[3] W.G. Etzkorn, S.E. Pedersen, T.E. Snead, Acrolein and Derivatives, John Wiley & Sons, Inc, 2000.
[4] National Research Council, Formaldehyde and Other Aldehydes, National Academy Press, 1981.
[5] K.H. Bowmer, G.H. Smith, Weed Res. 24 (3) (1984) 201–211.
[6] B. Cornils, in: H.F. Rase (Ed.), Handbook of Commercial Catalysts. Heterogeneous Catalysts, Angewandte Chemie International Edition, 2004.
[7] J.L. Callahan, R.K. Grasselli, E.C. Milberger, H. Arthur Strecker, Product R&D 9 (1970) 134–142.
[8] S. Kahlbum, Procédé de fabrication d'acroléine, FR 695931A (1930).
[9] J.-L. Dubois, C. Duquenne, W. Hoelderlich, Process for dehydrating glycerol to acrolein, WO2006087083A2 (2006).
[10] S. Erfle, U. Armbruster, U. Bentrup, A. Martin, A. Bruckner, Appl. Catal. A: Gen. 391 (1–2) (2011) 102–109.
[11] W. Suprun, M. Lutecki, T. Haber, H. Papp, J. Mol. Catal. A: Chem. 309 (1–2) (2009) 71–78.
[12] N. Pethan Rajan, G. Srinivasa Rao, V. Pavankumar, K.V.R. Chary, Catal. Sci. Technol. 4 (2014) 81–92.
[13] M. Dalil, D. Carnevali, J.-L. Dubois, G.S. Patience, Chem. Eng. J. 270 (0) (2015) 557–563.
[14] J.-L. Dubois, K. Okumura, Y. Kobayashi, R. Hiraoka, Improved process of dehydration reactions, WO2013017942A2 (2013).
[15] M. Kaarsholm, F. Joensen, J. Nerlov, R. Cenni, J. Chaouki, G.S. Patience, Chem. Eng. Sci. 62 (18–20) (2007) 5527–5532.
[16] X.-L. Yang, W.-L. Dai, C. Guo, H. Chen, Y. Cao, H. Li, H. He, K. Fan, J. Catal. 234 (2) (2005) 438–450, ISSN: 0021-9517.
[17] J. Mol. Catal. A: Chem. 304 (1–2) (2009) 52–57, ISSN: 1381-1169.
[18] D. Stosic, S. Bennici, J.-L. Couturier, J.-L. Dubois, A. Auroux, Catal. Commun. 17 (2012) 23–28, ISSN: 1566-7367.
[19] A. Alhanash, E.F. Kozhevnikova, I.V. Kozhevnikov, Appl. Catal. A: Gen. 378 (1) (2010) 11–18, ISSN: 0926-860X.
[20] G.S. Foo, D. Wei, D.S. Sholl, C. Sievers, ACS Catal. 4 (9) (2014) 3180–3192.
[21] B. Katryniok, S. Paul, M. Capron, C. Lancelot, V. Belliere-Baca, P. Rey, F. Dumeignil, Green Chem. 12 (2010) 1922–1925.
[22] F. Wang, J.-L. Dubois, W. Ueda, Appl. Catal. A: Gen. 376 (1–2) (2010) 25–32, ISSN: 0926-860X.
[23] A.K. Kinage, P.P. Upare, P. Kasinathan, Y.K. Hwang, J.-S. Chang, Catal. Commun. 11 (7) (2010) 620–623, ISSN: 1566-7367.
[24] K. Okumura, Y. Kaypbashi, R. Hiraoka, J.-L. Dubois, Improved process of dehydration reactions, WO2013018915A3 (2013).

[25] E. Tsukuda, S. Sato, R. Takahashi, T. Sodesawa, Catal. Commun. 8 (9) (2007) 1349–1353.
[26] H. Atia, U. Armbruster, A. Martin, J. Catal. 258 (1) (2008) 71–82.
[27] S.-H. Chai, H.-P. Wang, Y. Liang, B.-Q. Xu, Green Chem. 9 (2007) 1130–1136.
[28] L.G. Possato, R.N. Diniz, T. Garetto, S.H. Pulcinelli, C.V. Santilli, L. Martins, J. Catal. 300 (2013) 102–112, ISSN: 0021-9517.
[29] J.-L. Dubois, Sustainable glycerine dehydration to acrolein, Presented at American Oil Chemists Society (AOCS), San Antonio, USA, 2014.
[30] J.-L. Dubois, Plate-type reactor with in-situ injection, US20,140,094,617 (2011).
[31] J.-L. Dubois, Catalytic reaction with reverse-flow regeneration, US20,150,141,703 A1 (2012).